On the effects of the equilibrium model in gyrokinetic simulations: from s-α to diverted MHD equilibrium

Burckel A.[1], **Sauter O.**[1], **Angioni C.**[2], **Candy J.**[3], **Fable E.**[2] and **Lapillonne X.**[1]

[1] *Ecole Polytechnique Fédérale de Lausanne (EPFL), Centre de Recherches en Physique des Plasmas, Association EURATOM- Confédération Suisse, CH-1015 Lausanne, Switzerland*
[2] *Max-Planck-Institut für Plasmaphysik, IPP-EURATOM Association, D-85748 Garching bei München, Germany*
[3] *General Atomics, P.O. Box 85608, San Diego, California 92186, USA*

E-mail: `olivier.sauter@epfl.ch`

Abstract. In order to better identify the role of the magnetic topology on ITG and TEM instabilities, different MHD equilibria with increasing complexity are calculated using the CHEASE code [1]. We start from the geometry of the s-α cyclone benchmark case [2], consider the corresponding circular numerical equilibrium, and then successively add a non zero value of α consistent with the kinetic profiles, an elongation of 1.68, a triangularity of 0.15, and finally an up-down asymmetry corresponding to a single-null diverted geometry. This gives the opportunity to study separately the effect of each main characteristics of the equilibrium on microinstabilities in core plasmas. Linear local electrostatic gyrokinetic simulations of these different numerical equilibria and of their corresponding analytical descriptions (Miller-type representations [3]) are performed using the codes GS2 [4, 5] and GYRO[6]. It is observed that each modification of the equilibrium has an influence on the results of gyrokinetic simulations. The effect of the α parameter can compensate the stabilizing effect of an increase in the elongation. A comparison between the up-down symmetric shaped equilibrium and its corresponding diverted configuration show a non negligible effect on the growth rate of ITG and TEM turbulence. The comparison between the local Miller model and using a full equilibrium shows that it is mainly the indirect change of elongation in the plasma core which influences the results. The global aim is to provide well defined benchmark cases including real geometry and kinetic electrons physics, since this is not analyzed by the cyclone case. In addition, the goal is to define a procedure for testing of local simulations inspired by experimental constraints and results.

1. Introduction

The magnetic flux surface shape defines the geometry of the plasma considered in a gyrokinetic simulation. It is generally defined either using an analytical model or solving numerically the Grad-Shafranov equation to obtain the MHD equilibrium. There are still many gyrokinetic simulations which are based on the $s - \alpha$ model for the equilibrium and used to compare with experimental results. In addition, these simulations are usually local flux tube simulations in order to save CPU time. However experiments do use the stabilizing effects of plasma shaping. In addition, the comparison of local transport properties between different plasma regions inherently include a difference in plasma shaping. Therefore gyrokinetic simulations need to include the effective magnetic topology [7, 8], either through the Miller model [3] or coupled to

a full 2D MHD equilibrium representation. Therefore, before validation of experimental results can occur, code benchmarking including these features is necessary. The aim of this work is to provide a benchmark framework which builds upon the cyclone case [2], but which would include the main new physics assumption which are usually used in present simulations, namely kinetic electrons, toroidal geometry, consistent α and collisionality. In addition, electromagnetic effects should be tested, but this can be performed at a later stage. On top of this, we would like this framework to allow for the comparison between local and global simulations. In doing so, we shall see that it provides a framework for comparison with experiments as well.

There have been many valuable published results of comparison between gyrokinetic simulations and experimental results or of high level code benchmarking. We cannot review them here and our purpose is to add to these activities with a different point of view, which provides new physics insights while performing code benchmarking. The most recent benchmarking activity has used the cyclone base case and adiabatic electrons, for core transport benchmark [9] using nonlinear codes. In this paper we first test linear simulations, since one cannot expect quantitative analyses of nonlinear simulations if the linear results do not agree already. A first step is to go beyond the $s - \alpha$ model, both in terms of magnetic topology and of finite value of α. It was thought that using an $s - \alpha$ model would ease the benchmarking exercise, removing the difficulties of checking the implementation of the equilibrium interface in different codes. It was shown recently that it was actually not true and even the $s - \alpha$ model introduced discrepancies and errors [10]. These can lead to differences sufficient to bring doubt about one code's simulations. This was recently resolved with respect to the $\rho*$ scaling [11], but it shows that benchmarking including the full MHD equilibrium is a timely exercise. These recent results [11] also show that comparing global and local results are very useful.

It is well known that the effect of kinetic electrons on ITG is significant. In addition, a recent paper using a quasi-linear model has shown that the transition between ITG and TEM is very important to determine the zero particle flux stationary state and therefore for particle transport [12]. This is confirmed by nonlinear results [13, 14]. Therefore it is important to benchmark as well the treatment of kinetic electrons included in the codes, both the effect on the ITG and the transition point to the TEM. Since finite α [15, 16] and collisionality have significant effects on TEM, they should be included as well. In this paper, we shall discuss the inclusion of finite α, however the inclusion of collisionality effects will be studied at a later stage.

2. The five MHD equilibria and the s-α model

There are many choices that can be made to define various equilibria from the cyclone test case, which is local, circular and based on the s-α model with α=0. Since the cyclone case is based on DIII-D experimental results [17], we found interesting to aim towards an equilibrium equivalent to the actual experiment. The latter has $q_{95} = 3.8$, $\kappa = 1.68$, $I_p = 1.3$MA, $B_0 = 2.09$, $\beta_N = 1.85$, $Z_{\mathrm{eff}} = 2.3$ and we reconstructed the pressure profile from Fig. 5 of [17] as well, with $p_{\mathrm{edge}} = 0$. For the plasma boundary, we have taken a typical single-null (SN) from DIII-D and the above geometrical characteristics as seen in Fig. 1(e). To match the top triangularity, we have chosen $\delta = 0.15$. These choices allow to define five equilibria with increasing shaping effects from circular-$\alpha = 0$ (Fig. 1a), circular-$\alpha \neq 0$ (Fig. 1b), elongated (Fig. 1c), elongated+triangularity (Fig. 1d) and up-down asymmetric (Fig. 1e).

The q profile still needs to be determined. Since the central q value is usually close to one, experimentally, we imposed $q_0 = 0.95$. One could also impose the $q = 1$ radius, however matching q_0, q_{95} and the value of $q = 1.4$ and $s = 0.78$ at $r/a = 0.5$, as in the cyclone case, was sufficently constraining. This has been performed by tuning the current density profile given to the CHEASE equilibrium code [1]. The resulting flux surfaces are shown in Fig. 1, where $a = 0.36$ and $R_0 = 1.68$ was also used. The corresponding eqdsk files are available as output of the code. Note that both the q profile and the magnetic shear profiles do match very well for the

five equilibria. One could have chosen to keep I_p fixed. However experimental comparison across machines are usually performed at similar q_0 and q_{95} values and thus at similar q profile. Note also that we want to compare the ITG and TEM growth rates with local physics parameters as close to the cyclone base case as possible, in order to compare them within the same context. It should be noted that usually, when the plasma elongation is increased in particular, the q profile broadens and is essentially flat and near one over a large volume. However in the suite of equilibria computed here, we have kept the q profiles self-similar.

Table 1 gives the main parameters of these equilibria, with κ and δ being the local values of elongation and triangularity and not the edge values. The shift is defined by dR_0/dr where R_0 is the flux surface geometrical center.
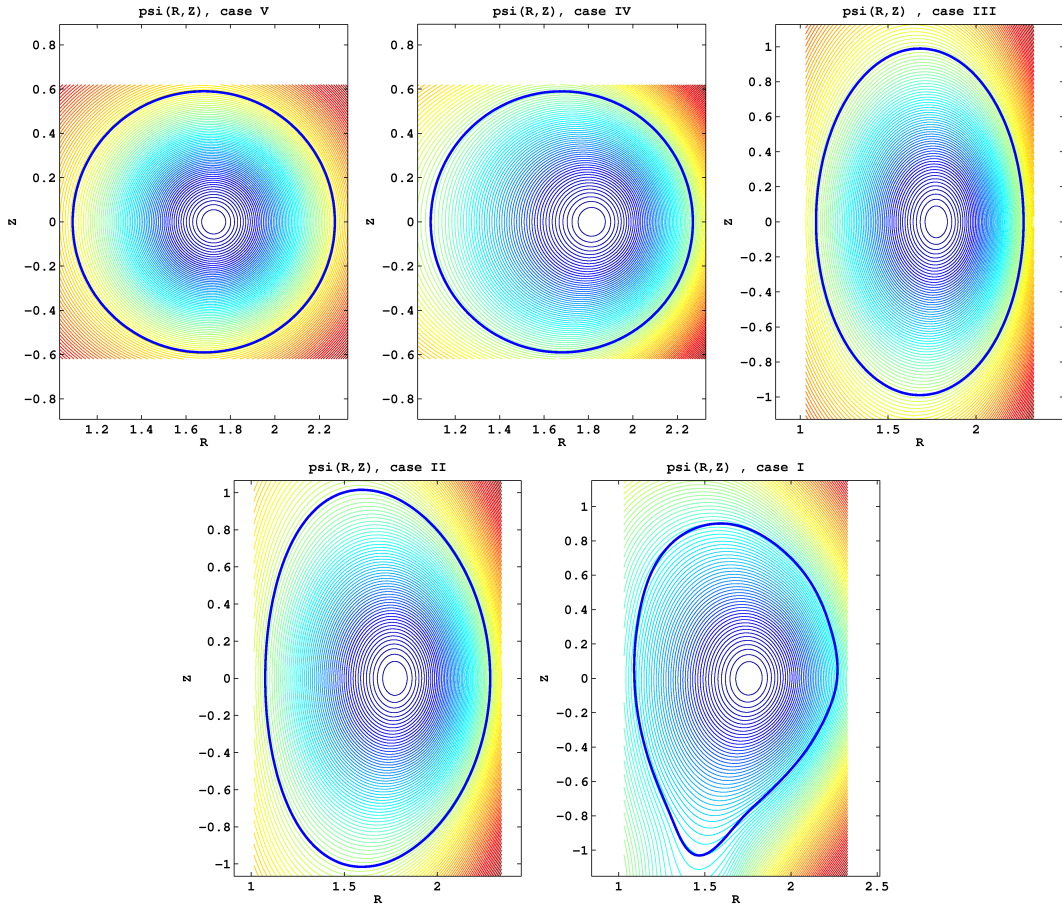

Figure 1. The five equilibria: (V) circular $\alpha = 0$; (IV) circular $\alpha \neq 0$; (III) elongated $\alpha \neq 0$; (II) $\kappa + \delta$ and $\alpha \neq 0$; (I) single-null down.

3. Some specifications about the simulations

Other parameters, non related directly to the magnetic topology are taken from cyclone case (based on DIII-D discharge 81499): $n_e = n_i$, $T_e = T_i$, $\epsilon_0 = \frac{r0}{R_0} = 0.18$, $r/a = 0.5$, R_0=1.68m, a=0.6m , R/L_n=2.22 ,R/L_T=6.91. These are the local values at $r/a = 0.5$, the full profiles are shown below. In this paper, only the local Eulerian gyrokinetic simulations have been performed with GS2 and GYRO.

number	shape	q	q_{95}	s	α	shift	κ	δ	I_p [MA]	β_N
V	circular	1.42	3.72	0.84	0.0	-0.06	1.01	0.00	0.64	0.0
IV	circular	1.45	3.66	0.76	**0.47**	-0.23	1.04	0.00	0.78	3.60
III	elongaged	1.38	3.70	0.74	0.49	-0.16	**1.47**	0.00	1.34	2.16
II	shaped	1.37	3.87	0.77	0.49	-0.16	1.43	**0.03**	1.33	2.18
I	**diverted**	1.37	3.92	0.80	0.48	-0.15	1.30	0.08	1.31	2.17
Exp.[17]	diverted	1.4	3.8	0.78	-	-	-	-	1.3	1.85

Table 1. Caracteristics of the 5 equilibria created to pass from a concentric circular geometry to a geometry close to an experimental discharge. The value of κ at the last closed flux surface is 1.68 and the value of δ is 0.15 .

In GS2, the Miller flux surface shape is given by (in normalized units):

$$R(r,\theta) = R_0(r) + r\,cos[\theta + \delta(r)sin(\theta)] \qquad (1)$$
$$Z(r,\theta) = \kappa(r)\,r\,sin(\theta) \qquad (2)$$

The Miller-type flux surface shape of GYRO is given by:

$$R(r,\theta) = R_0(r) + r\,cos(\theta + arcsin(\delta(r))sin(\theta)) \qquad (3)$$
$$Z(r,\theta) = Z_0(r) + \kappa(r)\,r\,sin(\theta + \zeta(r)sin(2\theta)) \qquad (4)$$

One can notice that $\delta_{GS2} = sin^{-1}(\delta_{GYRO})$. In both codes, $\kappa(r)$ and $\delta(r)$ are calculated using limited developments around r the flux surface considered. The codes also need in input $\kappa' = d\kappa/d(r/a)$ and $\delta' = d\delta/d(r/a)$. The values considered for the five cases are in table 2.

number	κ'	δ'
V	-0.015	0.002
IV	-0.050	0.007
III	0.205	-0.019
II	0.217	0.078
I	0.200	0.209

Table 2. Additional Miller parameters

The pressure profile used for the equilibrium reconstruction was based on the profiles presented in [17]. Using CHEASE input parameters, we can obtain from total pressure the n_e and T_e profiles, assuming $T_e = T_i$, $n_e = n_i$, $L_{ne}/L_{Te} = 3$, $T_{e0keV}/n_{e0keV} = 0.69$ and $p_e/p = 0.5$. In this way, we make sure the kinetic profiles are consistent with the total pressure used for the equilibrium. We obtain the profiles shown in Fig. 2. We also show the profiles of R/L_{ne}, R/L_{ne} and $\rho* = \rho_s/a$, with $c_s = \sqrt{T_e/m_i}$ and $\rho_s = c_s/\Omega_i$, assuming a deuterium plasma. The values near $r/a = 0.5$ are very close to the cyclone base case and thus can be used with global codes for realistic benchmarking. Note that with global codes, not only the profile gradients vary over the plasma radius, but also the $\rho*$ value. However, we have constructed the equilibrium such that the pressure profile is consistent with the local scalelengths at $r/a = 0.5$ used for the local calculations (within 10%). In addition, the q and magnetic shear profiles are very close to one another throughout the scan in equilibria as shown in Fig. 3. Therefore this set of equilibria and profiles is very well suited for global code benchmarking as well.
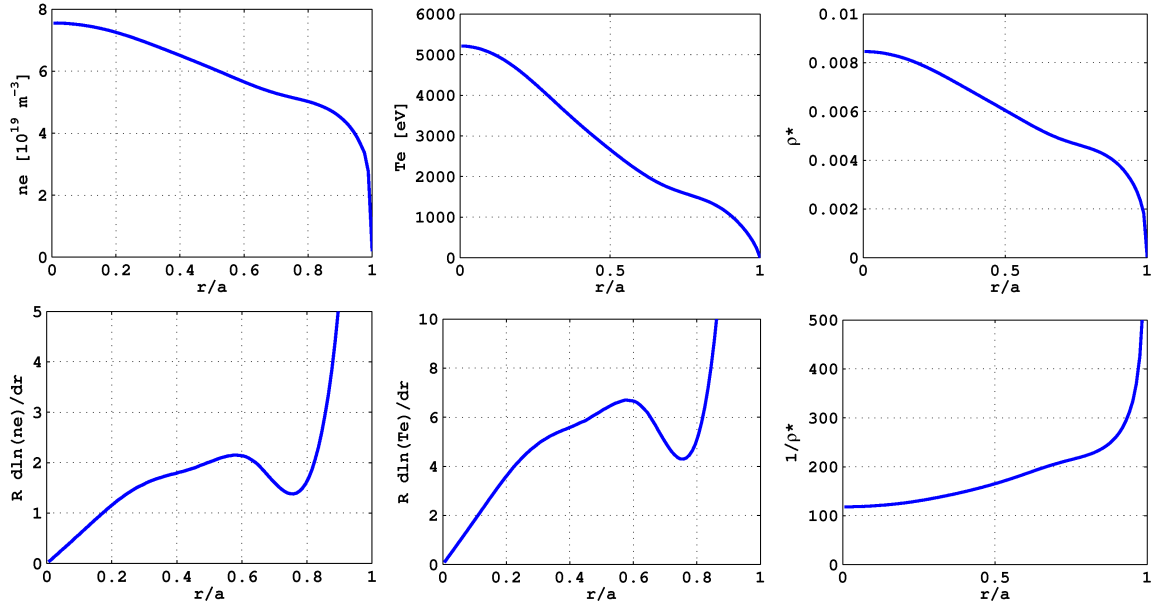
Figure 2. Profiles extracted from the pressure profile used for the equilibrium calculation with prescribed η and p_e/p with specific CHEASE input parameters.
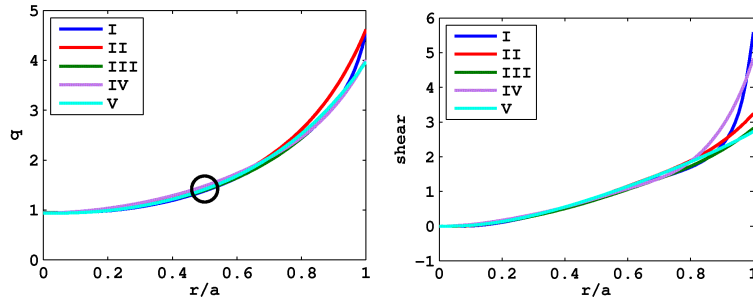

Figure 3. Safety factor q and magnetic shear s for the various equilibria.

4. Comparison of the three equilibrium models

There are basically three equilibrium models considered in this study: (1) the $s - \alpha$ model, (2) the Miller model, and (3) the full global MHD equilibrium. We compare these on the cyclone case, that is with $\alpha = 0$ and case V shown in Fig. 1. This is a similar comparison as performed in [10]. We find the same result, namely that the modes frequencies and growth rates obtained with the $s - \alpha$ model as implemented in GS2 and GYRO, does not match the ones obtained with a circular shaped configuration. The difference is explained in [10] and is due to an over-simplification of a metric term. On the other hand, both the Miller model and the full numerical equilibrium give the same results. In addition, for all cases, GS2 and GYRO give very similar results for both the ITG and the TEM branches. Note that the comparison performed here includes kinetic electrons, contrary to [2, 10]. It shows that the difference between the $s - \alpha$ model and the real geometry is not only with respect to the value of γ, but also the value of $k_y \rho_i$ at the transition between the ITG and TEM.

In Fig. 5, we compare these three equilibrium models with case IV as well, which has a finite

value of $\alpha = 0.5$. We find the same effects as with case V, $\alpha = 0$, Fig. 4. The value $\alpha = 0.5$ is such as to be consistent with the profiles corresponding to the input physics parameters $R/L_{n,T}$.
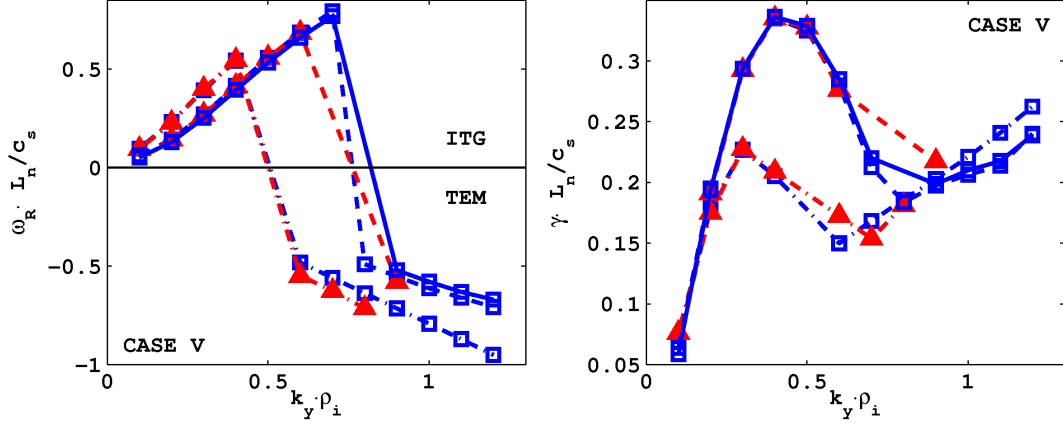

Figure 4. Real frequency (left) and growth rate (right) as a function of the poloidal wave vector k_y for a linear simulation of case V (Table 1). Solid line: numerical equilibrium, dashed line: Miller geometry and dashed-dotted line: $s - \alpha$ model. Red triangles: GYRO results, blue squares: GS2 results. The frequency follows GS2 convention, ion direction for $\omega > 0$.
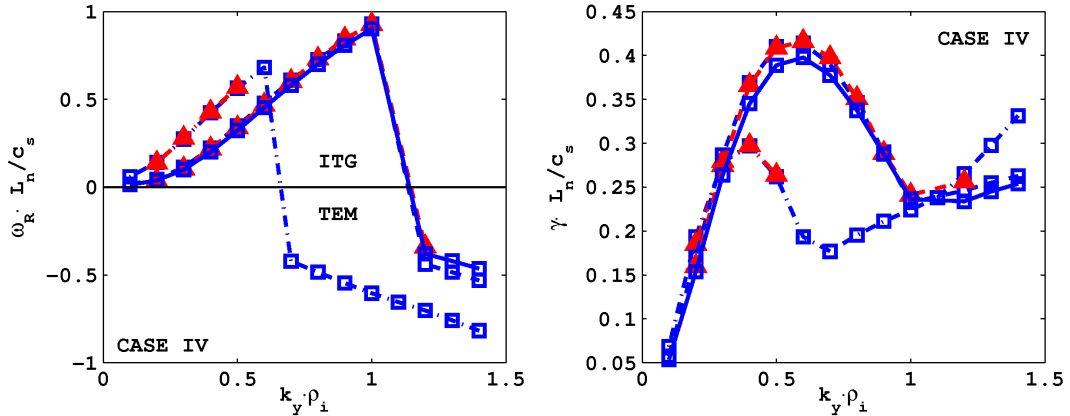

Figure 5. Same as in Fig. 4 but for the equilibrium case IV.

5. Miller and full equilibrium comparison at similar κ

In this Section we compare the Miller and numerical equilibrium models for the cases III, II and I, that is at fixed elongation and including finite δ, keeping up-down symmetry (case II), and including a full single-null down (SND) geometry with the same upper triangularity (case I). This is mainly to compare the codes with different equilibrium interface, within small modifications of the equilibrium, in order to have a better measure of the level of code and equilibrium model agreement.

Fig. 6 shows the modes frequencies and growth rates versus $k_y\rho_i$. Comparing solid lines (GS2-numerical equilibrium) with dashed lines (GS2-Miller), we see that there is essentially no

difference for the up-down symmetric cases and a small difference (about 5%) for the SND case. The GYRO results, with Miller, match very well the GS2 results as well, even for the SND case although the Miller representation is slightly different. We did not have time to compare with GYRO and the full MHD equilibrium and this will be performed at a later stage.

With respect to the influence of small shaping effects on the modes, we see that adding an edge $\delta = 0.15$ does not affect the modes much at mid-radius, as expected from Ref. [18]. On the other hand, the SND geometry has higher maximum growth rates. This is because the effective elongation decreases faster from the edge and is therefore smaller at $r/a = 0.5$ as seen in table 1. Since elongation is stabilising, this yields larger growth rates for the SND case. Note that with case I, there is a small difference between the Miller and numerical equilibrium, with GS2. This difference is larger than for cases II and III and is therefore significant. It is due to the non up-down symmetric shape of the flux surface, which can be encapsulated only with the numerical equilibrium, and the larger triangularity at the bottom. However the effect is small and Fig. 6 shows that the main parameter which needs to be matched is the flux surface elongation.
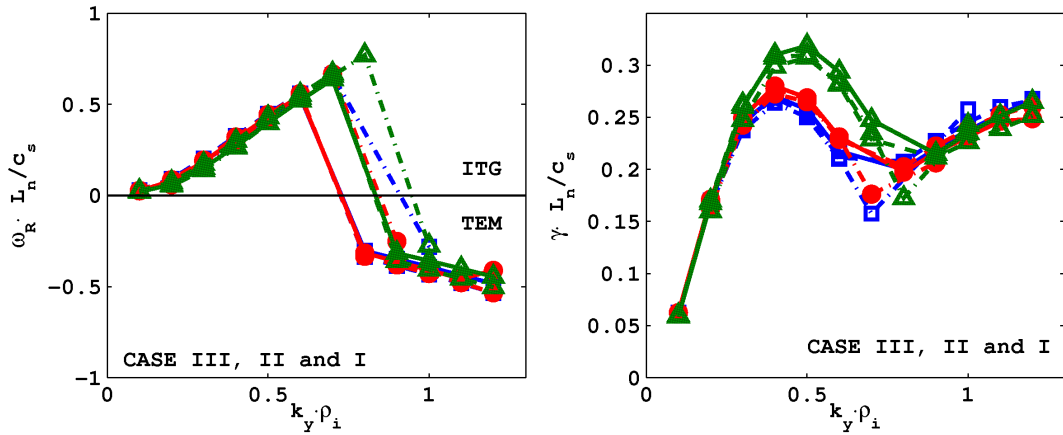

Figure 6. Real frequency (left) and growth rate (right) spectra for cases III (blue squares), II (red circles) and I (green triangles). Solid line: GS2 results with numerical equilibrium, dashed line: GS2 results with Miller geometry and dash-dotted line: GYRO results with Miller geometry.

6. From circular to single-null equilibria and the effects on ITG and TEM

We can now look at the general effects of shaping on the ITG and TEM modes when the global MHD equilibrium is modified from circular-non-shifted (V), to circular shifted (IV), to elongated-shifted (III), to elongated-shifted with triangularity (II) and finally to SND-shifted (I), while keeping the local value of ϵ, q and s constant as well as the global values of q_0 and q_{95}. This suite of equilibria mimics the various approximations performed when comparing with an actual experimental case (SND) and an "$s - \alpha$" equivalent case. Note that we do not compare with the $s - \alpha$ model since it is incomplete, as discussed above.

Fig. 7 shows the modes frequencies and growth rates versus $k_y\rho_i$ obtained with GS2 and the five numerical equilibria shown in Fig. 1. Comparing just the "experimental" case I and the simplest case V, circular-α=0, one could have concluded that there is little effects of shaping and no reason to use a realistic equilibrium. Indeed, both curves are nearby for both the frequency and the growth rate. However this is a coincidence and can be explained through the various steps. First, including a finite α value consistent with the imposed profiles, the modes are

destabilized. This is also somewhat coincidental since the effect of α can be either stabilizing or destabilizing depending on the magnetic shear as will be discussed below.

Adding elongation is strongly stabilizing and therefore the high growth rates of case IV are brought down by case III to the lowest values of the various cases (Fig. 7) and below the starting circular-α=0 case. The addition of positive triangularity, case II, only slightly destabilizes the modes, as discussed before. On the other hand, the final step, using a SND equilibrium which reduces the effective plasma elongation inside the plasma, is destabilizing and brings the growth rates back up to near the levels of the circular-$\alpha = 0$ case.
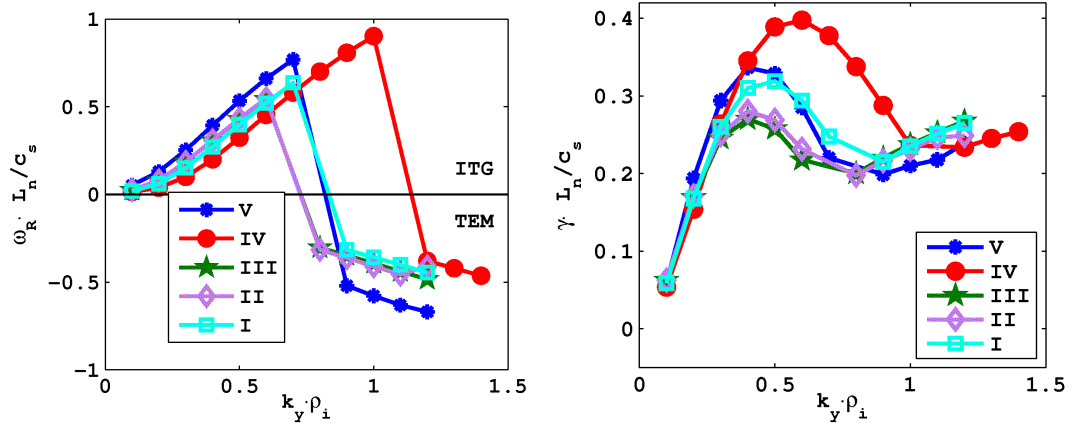

Figure 7. Real frequency (left) and growth rate (right) spectra for cases V, IV, III, II and I. Results obtained with GS2 and numerical equilibria.

The destabilization with α can be surprising since it is usually said that it is stabilizing. Actually, from the Ballooning representation one sees that it is $(s - \alpha)$ which is important. In addition, it is well known that the growth rate has a maximum near $(s - \alpha) = 0.5$. Therefore, depending on the starting parameters, increasing α can be either stabilizing or destabilizing, except if very large values of α are added, in which case it will be stabilizing. To have a better idea of the situation with this set of parameters, namely the cyclone case with kinetic electrons, we have performed a scan of shear and α values and determined the value of γ of the most unstable mode at $k_y\rho_i = 0.4$. The contour plot for the cyclone case with kinetic electrons and $s - \alpha$ model, for simplicity, is shown in Fig. 8(a). One clearly sees that not only the maximum value, but the whole contour lines align essentially along $(s - \alpha)$. The black line indicates that actually $s = 0.28 + 0.65\alpha$ reflects better the location of $\max(\gamma)$ at $k_y\rho_i = 0.4$. Assuming adiabatic electrons, we obtain almost the same slope for the ridge, namely $s = 0.37 + 0.63\alpha$. In Fig. 8(b), we show the case with $q = 2.84$ instead of $q = 1.42$. The fit changes slightly to $s = 0.315 + 0.70\alpha$, but the contours remain self-similar.

In Fig. 9 we then plot both γ and the mode frequency versus $(s - 0.65\alpha - 0.28)$, for various values of s, for the cyclone case with kinetic electrons. We see that all the curves align indeed very well and the offset of 0.28 is such as to bring the maximum γ's at $x = 0$. In this way one sees that the mode frequency is not at a minimum at this point. Of course, $(s - 0.5\alpha)$ would look almost as good, similarly to $(s - \alpha)$, which explains why either have been mentioned in the literature. The value of 0.65 is not universal and depends on the plasma parameters, as seen from the examples above. Note that the cyclone case has $s = 0.78$ and $\alpha = 0$, leading to $s - 0.65\alpha - 0.28 = 0.5 > 0$. This is why adding $\alpha = 0.5$, yielding $s - 0.65\alpha - 0.28 = 0.175$, one gets closer to the maximum and α is destabilizing. Figs. 8 and 9 show that the benchmark case
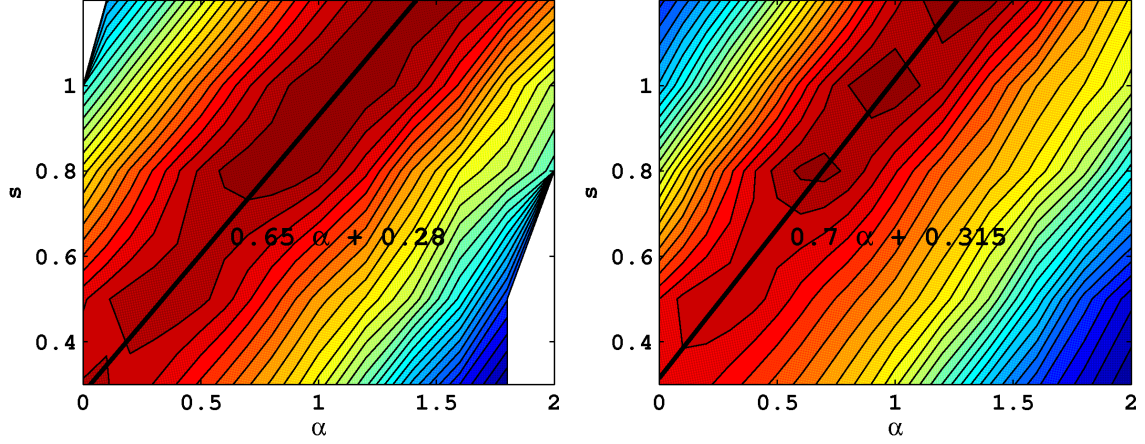
Figure 8. Contours of γ of the most unstable mode at $k_y \rho_i = 0.4$ for different values of s and α, using GS2 and the $s - \alpha$ model. (cyclone case with kinetic electrons and finite α. (b) same but with $q = 2.84$ instead of 1.42.

is close to the ridge and therefore small differences in the implementation of s or α in the codes might not be seen. Therefore, the comparison of a full scan is useful.
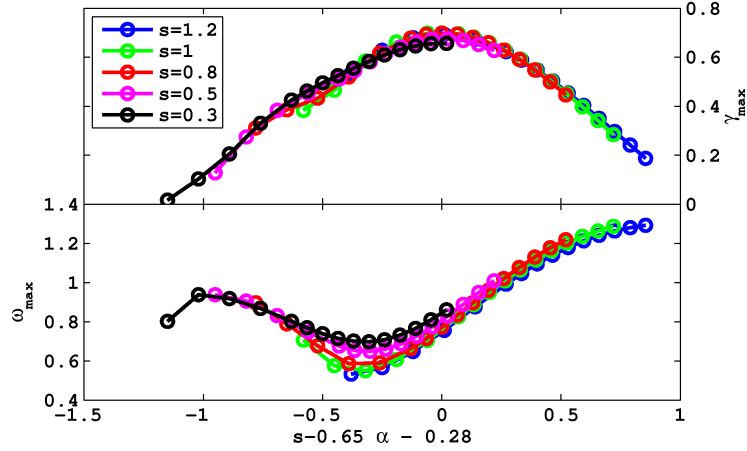

Figure 9. Growth rate (top) and real frequency (bottom) of the cases shown in Fig. 8(a).

7. Conclusion

We have extended the cyclone benchmark case [2] to include kinetic electrons, self-consistent finite α values and realistic magnetic geometry. This has lead to the construction of five equilibria in order to be able to compare with circular shape simulations (case V) up to full SND geometry (case I). The intermediate cases allow to check the equilibrium interface and to understand the effects of adding elongation, triangularity and up-down asymmetry. The calculation of the five equilibria is not unique. We have constrained the pressure profile to be consistent with the values of $R/L_{n,T}$ and with the original experimental data [17]. We have also imposed $q_0 = 0.95$

and the value of q_{95}, since this allows also to be closer to the comparison with experimental results.

We have analyzed the linear electrostatic results using the GS2 and GYRO codes, including three equilibrium models in the codes: $s - \alpha$, Miller [3], and MHD equilibrium (calculated with CHEASE in our case [1]). We have confirmed that the $s - \alpha$ model, as implemented in the codes, cannot reproduce the results with the circular non-shifted equilibrium (case V), as found in [10]. This difference remains important with kinetic electrons and finite α. We have also shown that both codes give similar results in all cases, and that the difference in the Miller model does not lead to significant differences with these parameters.

Both the ITG and TEM modes have been studied and their growth rates and mode frequencies vary with each equilibrium. Due to the original parameters of the cyclone case, adding a self-consistent α value to the circular equilibrium is destabilizing (case IV), while adding elongation is stabilizing (case III). The addition of triangularity on top of elongation (case II) has little effect and one would need a much larger triangularity to see a significant effect [18]. Finally, using a SND geometry (case I) with the same elongation and top triangularity as case II, is destabilizing. This is due to the reduction of the effective elongation of the core flux surfaces with respect to the up-down symmetric case. This could explain why double-null geometries tend to have better properties. In any case, it shows that the variations through these five equilibria are very instructive both for code benchmark purposes and to understand the effects of various assumptions when gyrokinetic simulations are applied to compare with experimental results.

These results and code comparisons are preliminary and for linear simulations only. The next step will be to compare nonlinear results. We have also only used local simulations, flux tube geometry at $r/a = 0.5$. However the framework of this set of equilibria and physics parameters are such as to allow the comparison with global simulations as well. The relevant files can be found in [19].

References
[1] H. Lütjens, A. Bondeson and O. Sauter, Comp. Phys. Comm. **97** (1996) 219.
[2] A. M. Dimits *et al*, Phys. Plasmas **7** (2000) 969.
[3] R. L. Miller *et al*, Phys. Plasmas **5** (1998) 973.
[4] M. Kotschenreuther, G. Rewoldt, and W. M. Tang, Comput. Phys. Commun. **88** (1995) 128.
[5] W. Dorland, F. Jenko, M. Kotschenreuther, and B. N. Rogers, Phys. Rev. Lett. **85** (2000) 5579.
[6] J. Candy, R.E. Waltz , J. Comp. Phys. **186** (2003) 545.
[7] E. A. Belli, G.W. Hammett, and W. Dorland, Phys. Plasmas **15** (2008) 092303.
[8] P. Angelino *et al*, Phys. Rev. Lett. **102** (2009) 195002.
[9] G. Falchetto *et al*, Plasma Phys. Contr. Fus. **50** (2008) 124015.
[10] X. Lapillonne *et al*, Phys. Plasmas **16** (2009) 1.
[11] B. F. McMillan *et al*, Phys. Rev. Lett., accepted (2010).
[12] E. Fable, C. Angioni and O. Sauter, Plasma Phys. Control. Fusion **52** (2010) 015007.
[13] T. Görler, Ph.D. thesis University of Ulm, Germany, 2009.
[14] X. Lapillonne *et al*, in Proc. of the 2010 Varenna-Lausanne conf., Journal Conf. Proc. Series 2010.
[15] C. Bourdelle *et al*, Nuclear Fusion **45** (2005) 110.
[16] A. Bottino *et al*, Plasma Phys. Control. Fusion **48** (2006) 215.
[17] C. M. Greenfield *et al*, Nuclear Fusion **37** (1997) 1215.
[18] A. Marinoni *et al*, Plasma Phys. Control. Fusion **51** (2009) 055016.
[19] http://crpp.epfl.ch/~sauter/benchmark